Naval Research Laboratory

Washington, DC 20375-5320

NRL/MR/6840--96-7810

Thermomechanical Effects in Metal Field Emitter Structures

M.G. ANCONA

Vacuum Electronic Branch
Electronics Science and Technology Division

March 22, 1996

REPORT DOCUMENTATION PAGE

Form Approved
OMB No. 0704-0188

1. AGENCY USE ONLY (*Leave Blank*)	2. REPORT DATE	3. REPORT TYPE AND DATES COVERED
	March 22, 1996	

4. TITLE AND SUBTITLE

Thermomechanical Effects in Metal Field Emitter Structures

5. FUNDING NUMBERS

PE - 0602234N
ONR - R534R54

6. AUTHOR(S)

M.G. Ancona

7. PERFORMING ORGANIZATION NAME(S) AND ADDRESS(ES)

Naval Research Laboratory
Washington, DC 20375-5320

8. PERFORMING ORGANIZATION REPORT NUMBER

NRL/MR/6840--96-7810

9. SPONSORING/MONITORING AGENCY NAME(S) AND ADDRESS(ES)

Office of Naval Research
Arlington, VA 22217-5000

10. SPONSORING/MONITORING AGENCY REPORT NUMBER

11. SUPPLEMENTARY NOTES

12a. DISTRIBUTION/AVAILABILITY STATEMENT

Approved for public release; distribution unlimited.

12b. DISTRIBUTION CODE

13. ABSTRACT (*Maximum 200 words*)

Analytical and numerical results concerning thermal and mechanical effects in operating metal field emitter structures (tips, gates and anodes) are summarized. For the most part, it is found that such effects are too small to constitute a reliability threat unless the geometries (via their effect on heat-sinking) or the operating frequencies (via their ac heating contribution) are extreme. For ideal structures of conventional (SRI-like) geometry under normal operating conditions the only two thermomechanical effects with the potential for triggering failure are i) anode heating due to electron impact and ii) Maxwell stress on the field emitter tip.

14. SUBJECT TERMS

Field emitter structures
Reliability
Thermal and mechanical effects
Maxwell stress
Nottingham heating

15. NUMBER OF PAGES

12

16. PRICE CODE

17. SECURITY CLASSIFICATION OF REPORT	18. SECURITY CLASSIFICATION OF THIS PAGE	19. SECURITY CLASSIFICATION OF ABSTRACT	20. LIMITATION OF ABSTRACT
UNCLASSIFIED	UNCLASSIFIED	UNCLASSIFIED	UL

NSN 7540-01-280-5500

Standard Form 298 (Rev. 2-89)
Prescribed by ANSI Std 239-18
298-102

CONTENTS

THERMOMECHANICAL EFFECTS IN METAL FIELD EMITTER STRUCTURES

INTRODUCTION

In this report, the thermomechanical state of field emitter structures under normal operating conditions (maximum dc currents less than about 0.1mA/tip) is analyzed. The structures examined are cylindrically-symmetric "SRI"-like field emitters [1] which are assumed to be defect-free and made of "linear" materials [2]. The tips are hyperboloids of varying sizes, sometimes sitting on posts, and the gates are coaxial rings. A typical cross-section is shown in Fig. 1. The thermomechanics of these structures is studied using simplified analytical models and by direct numerical simulation using the commercial finite-element code ABAQUS [3]. The equations solved are those of electrostatics, heat conduction and linear elasticity with temperature-dependent coefficients. And the emission currents and Nottingham heating are computed with the usual quasi-equilibrium, quasi-1-D Fowler-Nordheim equations [4]. The tip, gate and anode are assumed thermally and mechanically independent (e.g., gate heating does not produce tip heating) so that the calculations for each component can be performed *separately*; only the analysis of the tips has been published previously [5].

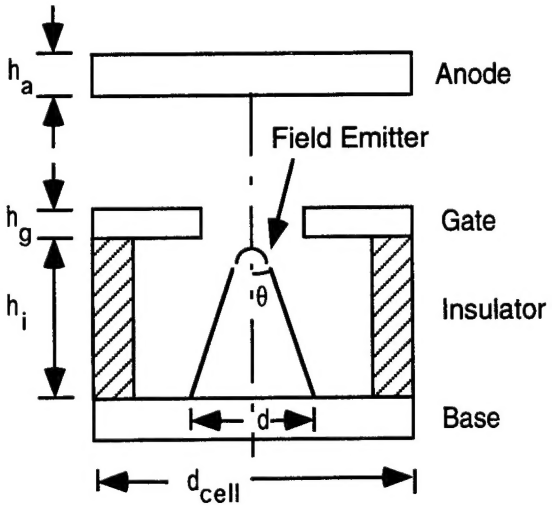

Fig. 1. Schematic of the "SRI"-like field emitter structure studied.

STEADY-STATE THERMAL RESULTS

Field Emitter Tips

The heat sources included in the tip analysis are ohmic heating associated with internal current flow and Nottingham heating associated with emission. Under normal operating conditions the Nottingham heating generally dominates as shown in Table 1 for a molybdenum tip with $\theta = 15^{\circ}$, an end radius of 200Å and $d = 0.4\mu m$. Note that because Nottingham heating increases linearly with current (Table 1) whereas ohmic heating goes as the square the latter could come to dominate but this occurs only at very high current levels [6]. Now the temperatures produced by this heating are strongly dependent on how well the tip conducts heat to the substrate (radiative loss is always negligible). This heat-sinking turns out to be excellent for most tips and so the tip temperatures typically remain near ambient as shown in Fig. 2 (for the tip of Table 1). Only when the currents are well beyond the normal operating range (>1mA, as might occur during an arcing failure) do the temperature excursions become appreciable (Fig. 2). To be more systematic, in Fig. 3 we summarize

Manuscript approved November 6, 1995.

the heat-sinking capability of tips as a thermal resistance [7]. Posts (of diameter d and height h) can also be characterized in this way and their resistances are shown in Fig. 3 as well [8]. To obtain the total thermal resistance of a tip-on-post structure one simply adds thermal resistances. As an example, for a tip-on-post structure with a post diameter of 0.4μm, post height of 1.6μm, cone half-

Current (mA)	Nottingham (mW)	Ohmic (μW)	Ratio (%)
0.01	0.004	0.00027	0.007
0.1	0.04	0.02	0.05
1.0	0.5	1.7	0.34
5.0	3.3	39.	1.2
11.	8.2	180.	2.2

Table. 1. Nottingham and ohmic contributions to the total heating as a function of current for a molybdenum tip. The former is seen to dominate.

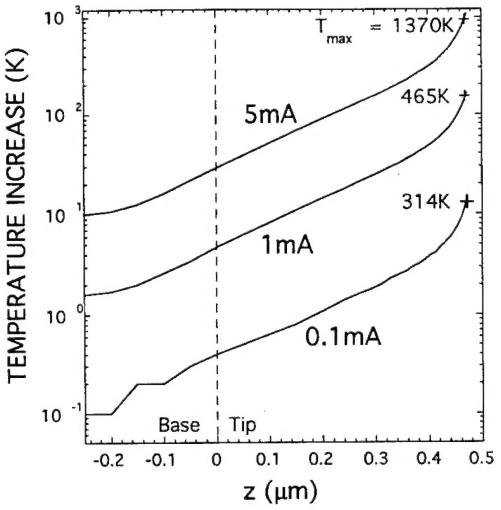

Fig. 2. Profile of the temperature increase above ambient along the centerline of the tip with current as a parameter.

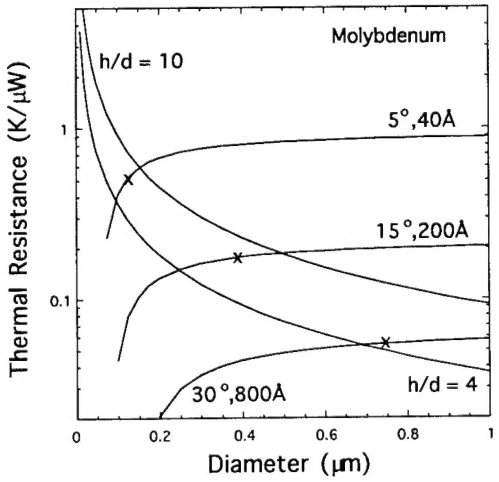

Fig. 3. Thermal resistance as a function of maximum diameter for three molybdenum tip geometries and two posts.

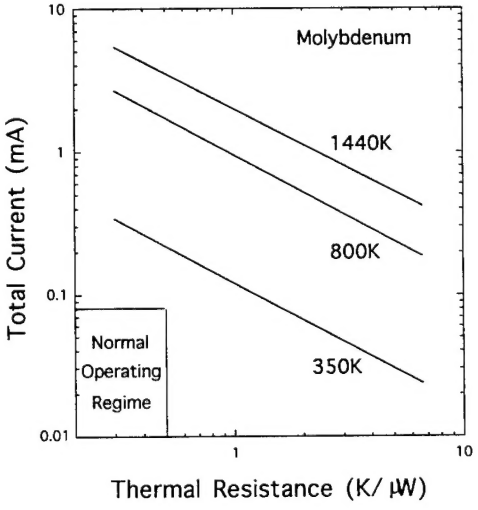

Fig. 4. Maximum tip temperatures for various combinations of current and thermal resistance.

angle of 15°, and end radius of curvature of 200Å, we have a total thermal resistance of 0.1 (post) + 0.18 (tip) = 0.28K/μW. The effect the heat-sinking capabilities (thermal resistances) of Fig. 3 have on tip temperatures is summarized in Fig. 4 where we plot the combinations of emission current (heating) and thermal resistance (heat-sinking) needed to produce several different temperatures [9]. The topmost curve gives the conditions under which the maximum tip temperature reaches half the melting point; this can be considered to define the thermal stability limit. Also shown in the figure is the normal operating regime for field emitter tips of "SRI"-like design (including the earlier example

with a thermal resistance of 0.28K/μW). Thus standard tips operate well within thermal limits and *it seems clear that under normal operating conditions thermal effects are unlikely to trigger molybdenum field emitters failure.* Only tips such as the "Eiffel tower" of Utsumi [10] with a thermal resistance of approximately 60K/μW might show thermal stability problems [9]. Finally, we note that identical calculations for tungsten yield very similar results with the tungsten running slightly cooler because of its 20% higher thermal conductivity.

A complete evaluation of the various assumptions behind this result (Fig. 4) is outside the scope of this report [5]. Nevertheless an indication of its robustness can be gleaned from the observation that, in simplest terms, the calculations of Nottingham heating produce an estimate of the average energy deposited per electron at the emitter surface. Combining this with the total current (known from experiment) then yields the heating. And given the heating one can calculate temperatures quite accurately. Thus errors due to effects of surface layers, inaccuracies in the Fowler-Nordheim analysis, etc. will largely be manifested as error in the deposited energy per electron. And a plot (Fig. 5) of the maximum tip temperature as a function of this energy (for tips of two geometries and at a current of 0.1mA) reveals that even if each electron deposits, on average, a very large and highly unlikely 3eV, the temperature excursions remain moderate. Hence, our conclusion that thermal effects are not likely to be the trigger for field emitter failure is a robust one.

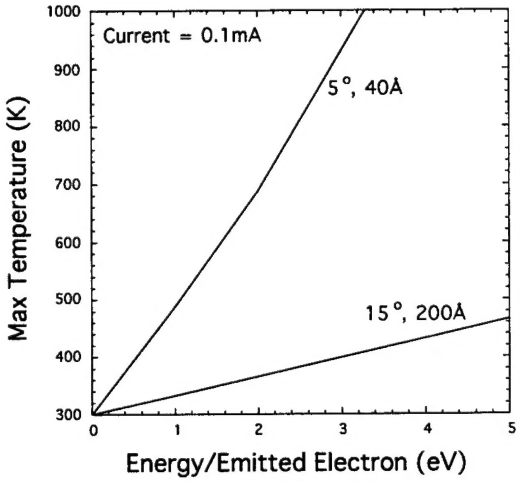

Fig. 5. Maxumum tip temperatures as a function of the energy deposited per electron at the surface for an emitted current of 0.1mA.

Field Emitter Gates

Heating of gates occurs primarily as a result of impact of energetic gate current electrons (ohmic heating is always negligible) but this heating does not produce significant temperature changes unless the heat sinking is poor. For a single annular gate separated from a conducting substrate by an insulating layer (Fig. 1), the maximum temperature excursion depends on whether there is significant heat sinking at the outer edge of the gate. The most interesting case is that of a large array with a single tip having an abnormally large intercepted current. For this case the edge heat sinking will be insignificant (unless the "bad" tip happened to be close to the edge) and most of the heat sinking will occur through the gate insulator. A plot of the temperature excursions obtained is shown in Fig. 6 [11]. As an example, if the design is that from Lincoln Laboratory [12] with $h_g = 0.05\mu m$ and $h_i = 0.2\mu m$ then the temperature rise due to a single emitter will be less than 50K per mW of dissipated power. This temperature does not seem anywhere near sufficient to trigger a localized breakdown (via thermal desorption). And, in general, we conclude from Fig. 6 that gate current from a single "bad" tip is not likely to thermally trigger arcing unless the gate currents are very high or the gates are ultra-thin.

A related case is that of a field emitter array with the gate current per tip being quasi-uniform over the array. For this case the expression from simple theory is approximately [13]

$$\Delta T_{max} \approx \frac{h_i V I_{gate}^{ave}}{d_{cell}^2 \kappa_i}, \qquad \text{(impact heating with uniform gate current)}$$

where h_i is the insulator thickness, d_{cell} is the spacing between tips (Fig. 1), κ_i is the thermal conductivity of the insulator and VI_{gate}^{ave} is the average power dissipated per tip. This equation is plotted in Fig. 7. Taking the Lincoln Laboratory [12] example again (h_i = 0.2μm, d_{cell} = 0.32μm) we have a maximum temperature rise of 1.4K per μW of average dissipated power (per tip). Since the average power dissipated is generally smaller than 50μW the temperature rise is insignificant (<70K) and again not likely to trigger arcing failure (much less melting).

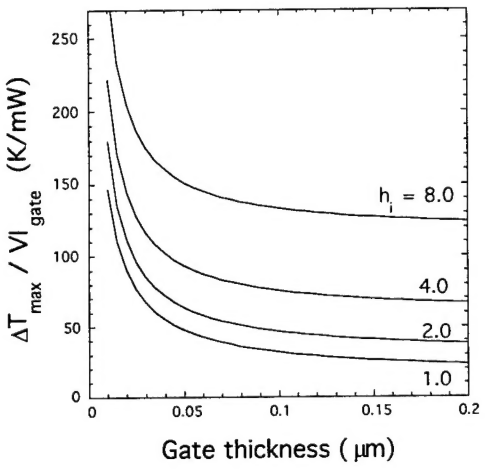

Fig. 6. Temperature excursions in single field emitter gate with no edge heat-sinking. VI_{gate} is the dissipated power in the gate and h_i is the insulator thickness.

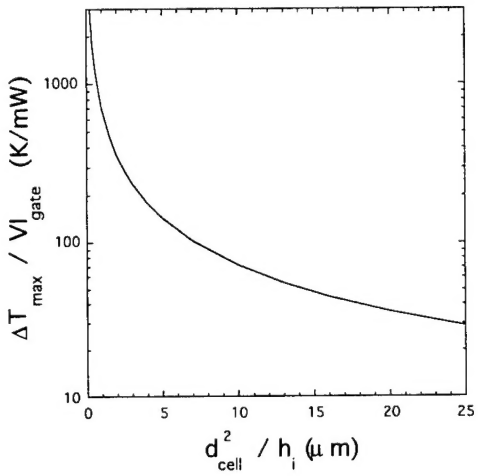

Fig. 7. Temperature excursions in gate structures of field emitter *arrays* as function of geometry.

Field Emitter Anodes

As with gates, the primary source of heat in anodes is associated with impact of the emission current electrons (ohmic heating is again negligible in steady-state). Considering a single circular anode of thickness h_a (see Fig. 1) which is shared by N field emitters with a total anode current of NI_{tip} one finds the maximum temperature excursion (at the anode center) due to electron impact heating to be

$$\Delta T_{max} = \frac{VI_{tip}N}{4\pi h_a \kappa} = 0.58\frac{VI_{tip}N}{h_a}, \qquad \text{(electron impact on anode)}$$

where V is the anode-to-cathode voltage and, in the second expression, V is in KV, I_{tip} is in μA, h_a is in μm and κ is assumed that for molybdenum at 300K. Evidently, anode heating resulting from electron impact can lead to a serious thermal problem especially if the anode is thin. As an example, if N = 1000, I_{tip} = 10μA, V = 100V and h_a = 0.5μm then T_{max} is roughly one-half the melting point of molybdenum. Thus our analysis suggests that anodes are more susceptible than gates to thermal instabilities. This greater susceptibility results from the currents being larger and because in our FEA model (Fig. 1) the anode makes thermal contact only at its outer edges whereas the gate can conduct directly to the substrate through the gate insulator.

AC AND TRANSIENT THERMAL EFFECTS

To understand the thermal behavior under ac/transient conditions the thermal time constants of the field emitter structure must be known. These vary inversely with size and can be estimated either by computing numerically the response to a step change in heating or by finding R_TC_T where R_T and C_T are the thermal resistance and capacitance, respectively. In Fig. 8 we show a numerically computed thermal transient for a tip with design like that assumed in Table 1 and Fig. 2. From this transient we determine a thermal time constant of about

$$\tau_{tip} \approx 3\text{nsec} .$$

The estimate based on the thermal resistance and capacitance is a somewhat larger 37nsec. For a post the thermal time constant (found from R_TC_T) is approximately

$$\tau_{post} = \frac{2\rho_m c_v hd}{3\kappa} \cong 12.3hd \text{ nsec} ,$$

where ρ_m is the mass density, c_v is the specific heat and the latter equality assumes molybdenum values and that h and d are in microns. The thermal time constant of an anode is roughly

$$\tau_{anode} \approx \frac{\rho_m c_v R^2}{\kappa} \cong 4.6R^2 \text{ nsec} ,$$

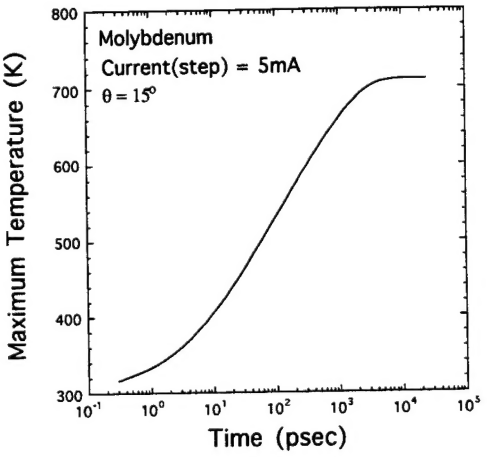

Fig. 8. Maxumum tip temperature as a function of time in response to a step change in tip current. The plot indicates a thermal time constant of about 3nsec.

where R is the outer radius and the latter expression again assumes molybdenum values and that R is in microns. And finally, the thermal time constant of the gate structure of an FEA is roughly

$$\tau_{gate} \approx \frac{\rho_m c_v h_i h_g}{\kappa_i} \cong 1.8h_i h_g \ \mu\text{sec} ,$$

where the latter assumes the gate to be molybdenum, the insulator to be SiO_2 and h_g and h_i to be in microns. Not surprisingly, the time constants of the anode and the gate are much longer than those of the field emitter itself and thus the entire FEA has thermal time constants which vary from 3-1000+ nsec or, equivalently, response frequencies which range over <1-300MHz. And since the relevant frequencies for applications of field emitters range from kHz (displays) to GHz (microwave devices) one can expect FEAs to exhibit both low and high frequency thermal behaviors. In the high-frequency limit the temperatures would simply be characteristic of the *average* heating and so will be equivalent to dc results reduced by the duty cycle. This case is obviously well-modeled by the dc results. In the low-frequency limit, the temperatures *follow* the time-varying heating in a quasi-dc manner. And again this is well-modeled by the dc case although the increased thermal cycling may have consequences for reliability.

Some ac/transient *electrical* effects are also relevant to understanding the ac/transient *thermal* behavior. The only such effect considered here is the additional ohmic heating that can occur in association with ac currents [14]. This effect is readily estimated and, as seen below, is usually insignificant. For a tip, a dc current of 0.1mA would have thermal impact if the ohmic heating was increased by roughly 5 orders of magnitude. This suggests that thermal effects would enter if the ac current were larger than about 30mA (= 0.1mA x $10^{5/2}$). Assuming a single-tip capacitance of 2fF and a voltage swing of 50V this implies a frequency of 5GHz. Thus thermal effects in the tip may be

important but only for the highest frequency applications. For an anode of thickness h and capacitance C_{anode} the maximum temperature excursion due to ac ohmic heating (assuming the current flow is radial) is approximately

$$\Delta T_{max} = \frac{\rho}{64\kappa}\left(\frac{fC_{anode}\Delta V}{h}\right)^2 = 6x10^{-6}\left(\frac{fC_{anode}\Delta V}{h}\right)^2 , \qquad \text{(ac heating of anode)}$$

where f is the driving frequency, ΔV is the ac voltage swing and the second equality follows for molybdenum with f in GHz, C_{anode} in pF, ΔV in volts and h in μm. This is generally small unless the anode is very thin or the voltage swing is overly large. A similar conclusion holds for gates associated with individual tips. And lastly, for an FEA gate structure the approximate maximum temperature excursion is

$$\Delta T_{max} = \frac{\rho\kappa_g}{\kappa_i^2}\left(\frac{\pi fC_{tg}\Delta Vh_i}{d_{tip}^2}\right)^2 \cong 36.1\left(\frac{fC_{tg}\Delta Vh_i}{d_{tip}^2}\right)^2 , \qquad \text{(ac heating of FEA gate)}$$

where C_{tg} is the tip-to-gate capacitance of a single tip and again the second equality follows for molybdenum with f in GHz, C_{tg} in pF, ΔV in volts and the distances in μm. This too is almost always small.

MECHANICAL RESULTS

The minimal temperature rises that occur in operating field emitters (see above) mean that thermal stresses in the tips will be small (typically more than two orders of magnitude below the yield strength). We also ignore possibly large intrinsic stresses. Therefore, as in the field-ion microscope [15], the stress state in the field emitter is dominated by Maxwell (electrostatic) stresses produced by the extremely high electric fields. From a plot (Fig. 9) of these stresses (the on-axis tensile component at the tip apex is shown) as a function of the electric field (also at the apex) it is seen that when the electric field exceeds 1V/Å the stress at the tip approaches the bulk yield strength of molybdenum. Since fields of this magnitude are seen in normal operation this figure suggests that Maxwell stress could impact reliability, possibly leading to improvement ("seasoning"), e.g., by field-

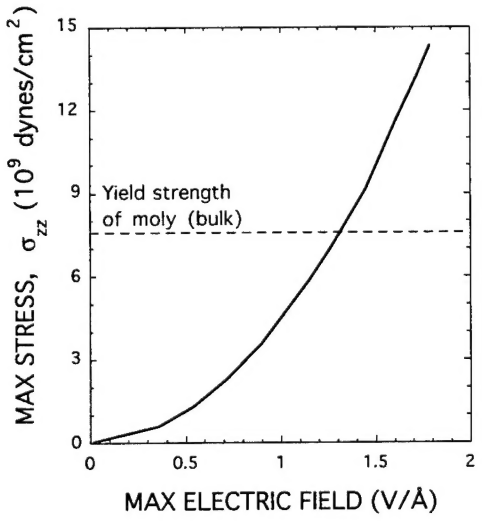

Fig. 9. Maximum tensile stress at the tip apex as a function of the electric field at the apex due to Maxwell forces.

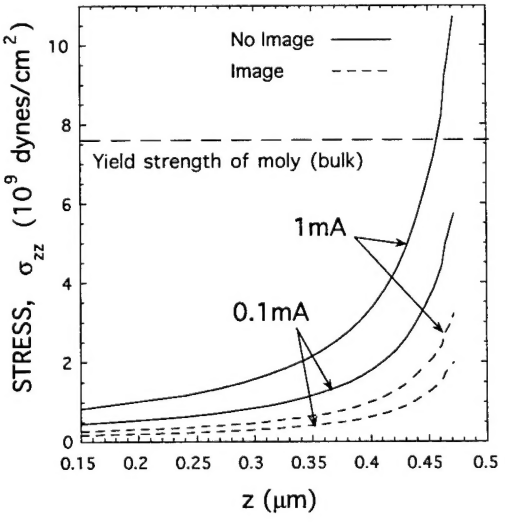

Fig. 10. Tensile stress profiles in a tip for various currents and with and without image force effects.

aided surface diffusion, or to mechanical failure. Unfortunately, firmer conclusions are impossible due to various uncertainties. First, mechanical properties are not well-known even in bulk materials (the bulk tensile strength varies from 4.4-13.8 x 10^9 dynes/cm^2 [2]) and are sensitively dependent on defects, impurities and temperature [16]. And secondly the electric fields actually present at the tip apex are strongly-dependent on details of Fowler-Nordheim theory [17]. In this regard, whether or not an image force should be included in the analysis [18] can have a significant impact on the stress as shown in Fig. 10. Finally, we note that since both temperatures *and* electric fields are relatively low at anodes and gates the stresses in these structures (apart from intrinsic stresses) will be relatively low.

Acknowledgements: The author thanks Drs. H.F. Gray, J. Shaw, P. Phillips and K. Jensen for many useful discussions, Ms. J. Sun for assistance in the gate heating calculations and NRL's Vacuum Electronics Branch (Dr. R. Parker, Head) for funding support.

REFERENCES

1. Such structures are currently being fabricated not only by SRI International but also by LETI, PIXEL International, MIT Lincoln Laboratory, Micron Technology and others.

2. T.E. Tietz and J.W. Wilson, Behavior and Properties of Refractory Metals, (Arnold, London, 1965).

3. Hibbitt, Karlsson and Sorenson, Inc., Pawtucket, RI. Version 5.3.

4. A. Modinos, Field, Thermionic and Secondary Electron Emission Spectroscopy, (Plenum, New York, 1984).

5. M.G. Ancona, to be published, *J. Vac. Sci. Tech.* (1995). Note that the electrostatics is coupled but that, for simplicity, has been computed assuming no gate.

6. G.N. Fursey and D. Glazanov, *J. Vac. Sci. Tech.* **B13**, 1044 (1995).

7. The heat-sinking of a tip can be described as a simple thermal resistance only because the Nottingham heating is concentrated at the apex of the tip (where the emission occurs). For the plot the tip thermal resistances (for three tips with different cone angles and end radii of curvature indicated in the figure) were computed numerically only at the points denoted by "X"'s. At these points the thermal resistance was found to vary by less than 20% as a function of current. The curves extrapolating away from these points were obtained using the "hollow sphere" formula

$$R_{tip} = R_x + \frac{d/\sin\theta - 2d_x}{\kappa\pi d d_x \sin\theta}$$

where d is the base diameter, the thermal conductivity κ was taken to have its room temperature value and the x subscripts indicate "X"-point values. This formula becomes increasingly invalid for small diameters (in fact, it eventually goes negative) but should be reasonable for larger diameters.

8. The post thermal resistances were computed from $R_{post} = 4h/(\kappa\pi d^2)$ where h is the post height and κ is taken to have its room temperature value.

9. The lines in this Figure can be extrapolated so long as the currents are not so large as to make ohmic heating significant. (Consequently this Figure is not relevant to very high current situations like those discussed in Ref. 6).

10. T. Utsumi, *IEEE Trans. Elect. Dev.* **ED-38**, 2276 (1991).

11. Treating an annular gate of inner radius R_1, outer radius R_2, thickness h_g and thermal conductivity κ_g two limiting cases are readily analyzed: with perfect heat sinking at the outer edges ($r = R_2$), i.e., with the edge held at 300K, and with no heat sinking there. The formulas that result are

$$\Delta T_{max} = \gamma \frac{I_o(r_2)K_o(r_1) - I_o(r_1)K_o(r_2)}{I_o(r_2)K_1(r_1) + I_1(r_1)K_o(r_2)}, \qquad \text{(perfect edge heat sinking)}$$

$$\Delta T_{max} = \gamma \frac{I_o(r_1)K_1(r_2) + I_o(r_1)K_o(r_2)}{I_1(r_2)K_1(r_1) - I_1(r_1)K_1(r_2)}, \qquad \text{(no edge heat sinking)}$$

where

$$\gamma \equiv \frac{VI_{gate}}{2\pi R_1}\sqrt{\frac{\kappa_i \kappa_g h_g}{h_i}} \quad , \quad r_{1,2} \equiv R_{1,2}\sqrt{\frac{\kappa_i}{\kappa_g h_g h_i}} \quad ,$$

I_{gate} is the gate current, V is the gate-to-tip voltage and I_n and K_n are modified Bessel functions. In the former case, the temperature excursions are never large (for any realistic dimensions); the latter case was discussed in connection with Fig. 6.

12. C. Bozler, D. Rathman, C. Harris, G. Lincoln, R. Mathews, S. Rabe, R. Murphy, M. Hollis and H. Smith, *Int. Vac. Microelect. Conf. Tech. Dig.*, 118 (1995).

13. A more accurate expression for impact heating of an FEA gate due to quasi-uniform gate current is

$$\Delta T_{max} = \frac{h_i V I_{gate}^{ave}}{d_{cell}^2 \kappa_i}\left[1 - \frac{1}{I_o\left(d_{cell}\sqrt{\kappa_i N/(\pi \kappa_g h_i h_g)}\right)}\right].$$

The expression given in the text and plotted in Fig. 7 results when the heat-sinking is dominated by conduction through the insulator (rather than to the outer edges).

14. Some ac effects whose impact on the thermal problem we presume negligible are those associated with RC charging times and with the skin effect.

15. K.D. Rendulic and E.W. Muller, *J. Appl. Phys.* **38**, 2070 (1967); P.J. Smith and D.A. Smith, *Phil. Mag.* **19**, 907 (1970).

16. An example of the possible complications involved is that the materials of interest undergo brittle-to-ductile transitions at moderate temperatures (for moly the transition occurs around 300K while for tungsten the transition is around 500K [2]).

17. The electric fields at the tip are also strongly-dependent on the unknown tip curvature. However, the electric field needed to produce a given emitted current is relatively independent of curvature so this is not a great source of uncertainty.

18. Calculations by the author [M.G. Ancona, *Phys. Rev.* **B46**, 4874 (1992)] suggest that, contrary to conventional belief, greater accuracy is obtained by ignoring the image force "correction."